Double Electron-Electron Resonance

Distance Distribution Modeling in Spin Systems using Electron Spin Spectroscopy

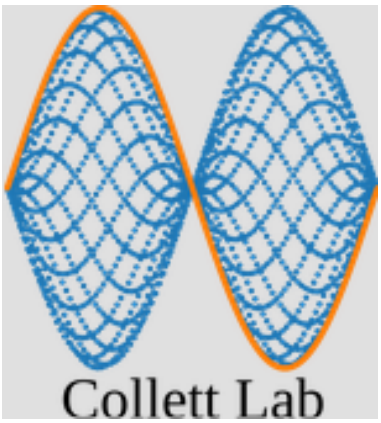

Nina Neumann

A thesis submitted in partial fulfillment of the requirements for

Bachelor of Arts in Physics

Faculty Advisor: Professor Charles Collett

Department of Physics

Hamilton College

August 25, 2025

Abstract

Free radicals—molecules with unpaired electron spins—play a key role in many biological processes due to their high reactivity, as unpaired electrons tend to seek pairing through chemical interactions.[1] Pulsed electron-electron double resonance (PELDOR/DEER) spectroscopy is a powerful method for measuring nanometer-scale distances between unpaired electron spins in biological systems. In this senior project, we simulate a four-pulse DEER sequence on a two-spin model with varying precession rates to examine how dipolar coupling signals and their time evolution relate to inter-spin distances. By varying the timing of a selective π pulse on a simulated spin ensemble and fitting the resulting echo signal, we extract a characteristic oscillation frequency that is directly tied to the dipolar coupling of the system. The methods described allow for distance extraction from simulated time dependent data.

1 Acknowledgments

I would like to thank my advisor, Professor Charles Collett, for his support and guidance throughout this project. I'm also grateful to the Hamilton College Physics Department—not only for their academic support, but for fostering an environment that has become a home to me over these past four years. It's through this department that I've made some of my closest friendships, which I hope to carry with me for a lifetime. To my friends and family, thank you for your patience and encouragement—this would not have been possible without your support, both in the classroom and beyond. This project—and my time at Hamilton—would not have been the same without the people who shaped it. I could not be more fortunate to have shared this time with such a strong and supportive community.

Contents

1 Acknowledgments **2**

2 Introduction **4**

3 Background **5**

4 Theory **8**

4.1 Hamiltonian 8

4.2 Zeeman interaction term 8

4.3 RF Hamiltonian for ESR 9

4.4 Rotating Wave Approximation (RWA) 9

4.5 Decoherence 10

4.6 Dipolar Interaction Term 12

5 Methods **14**

5.1 Pulse Sequence 14

5.2 Bloch Sphere time evolution 15

5.3 Qutip Simulation Framework 16

5.4 Dipolar Interaction and Distance Extraction 17

6 Results **18**

6.1 V(T) modulation from dipolar coupling 18

7 Discussion **20**

8 Conclusion **22**

A Code Listings **23**

A.1 Pulse and Evolution Functions 23

A.2 V(T) Curve Generation 23

2 Introduction

Magnetic resonance techniques—including Nuclear Magnetic Resonance (NMR) and Electron Spin Resonance (ESR)—are powerful tools for probing atomic-scale properties across a range of scientific and medical disciplines. NMR has become essential in applications such as medical imaging and structural biology, offering non-invasive, atomic-level insights into molecular systems through techniques like Magnetic Resonance Imaging (MRI).[2] While NMR focuses on nuclei with magnetic moments, ESR is uniquely suited for studying systems containing unpaired electron spins, including free radicals—molecules with unpaired electrons—transition metal complexes, and paramagnetic centers. These species are key players in biological processes such as oxidative stress, metal ion coordination, and enzymatic activity.[3,4]

Both techniques rely on the same core principle: using an external oscillating magnetic field to drive transitions between spin states. However, ESR is particularly sensitive to the local environment of unpaired electrons and enables direct measurement of spin-spin interactions and nanometer-scale structural features.

A major strength of ESR is its ability to quantify distances between electron spins, making it invaluable in structural biology. This is especially true for nanometer range distance measurements, whereas traditional NMR methods often lack this level of sensitivity. Techniques such as Double Electron-Electron Resonance (DEER) leverage dipolar interactions between spins to extract precise distance distributions.[4]

In this project, we investigate how ESR—specifically DEER spectroscopy—can be used to extract structural information from biological molecules. By modeling spin interactions with spin Hamiltonians and simulating their dynamics using the Quantum Toolbox in Python (QuTiP), we aim to demonstrate how DEER enables high-resolution distance measurements between spin labels that can also be used for biological systems. These methods can also be used for more basic characterization of inter-spin couplings, which has applications for our research group more broadly.

3 Background

Electron Spin Resonance (ESR), also known as Electron Paramagnetic Resonance (EPR), is a magnetic resonance technique that detects unpaired electron spins in a system. Much like Nuclear Magnetic Resonance (NMR), ESR looks at the interaction between magnetic fields and quantum spin states. However, where NMR focuses on atomic nuclei, ESR probes electrons directly. This is significant because electrons have significantly larger magnetic moments and thus respond to higher-frequency radiation than their nuclear counterparts. As mentioned previously, this makes ESR particularly well-suited for studying free radicals, transition metal ions, and paramagnetic centers, all of which play key roles in many biological processes.[3,4]

When an external magnetic field (B_0) is applied, the magnetic moments of unpaired electrons align either parallel or antiparallel to the field, corresponding to two distinct energy levels—commonly referred to as spin-up and spin-down states. Transitions between these levels can be induced by applying electromagnetic radiation at the resonance frequency, which produces signals detectable as ESR spectra. In quantum mechanical terms, however, electron spins are not restricted to being strictly up or down; they can exist in coherent superpositions of these two states. As will be further discussed in the methods section, this superposition can conveniently visualized using the Bloch sphere which represents the full quantum state of a spin-1/2 particle and also helps illustrate how external pulses can modulate spin orientation during ESR experiments.

ESR is commonly implemented in two modes: continuous-wave (CW) ESR, where a constant microwave frequency is applied, and pulsed ESR, which uses short but strong microwave pulses to look at spin dynamics over time. This thesis focuses on pulsed ESR, as it enables precise measurements of spin interactions and distance-dependent couplings through time-dependent pulse sequences such as Double Electron-Electron Resonance (DEER) which will be discussed at length in later sections.

ESR has unique capabilities in biomedical research due to its high sensitivity to unpaired electrons. Free radicals play an essential role in many physiological processes and pathological conditions. One of the most significant roles is in the mechanism of oxidative stress. This is a physiological process characterized by an imbalance between the production of reactive oxygen species (oxygen-containing free radicals) and the rate at which the body can neutralize them.[5]

Reactive oxygen species typically contain large numbers of free radicals which is why they are so chemically unstable. Normally, the body can maintain equilibrium; however, when too many are produced too quickly, the resultant oxidative stress can cause significant damage to important parts of our cells such as DNA and encoding proteins.[6] Chronic oxidative stress is associated with a number of diseases, including neurodegenerative diseases such as Alzheimers, diabetes, and cancer progression. For one, tumors often exist

in oxygen deprived environments. ESR-based oximetry can monitor oxygen and radical species concentrations in living subjects which is critical to understanding key treatment tenets such as tumor metabolism, chemotherapy resistance, and drug delivery.

Another useful role for oxygen sensitivity is during a stroke or similar ischemic events where living tissues are deprived of oxygen. When blood flow is restored, an excess of reactive oxygen species are produced which exacerbates the hypoxia-induced tissue damage.[6] In pulmonary conditions such as chronic obstructive pulmonary disease (COPD) and asthma, reactive oxygen species also play a key role in inflammatory signaling.

Recent experiments have also looked into ESR-based probes and spin labels that can be inhaled as a possible measurement mechanism for the oxidative burden in lung tissues. ESR oximetry leverages the paramagnetic properties of molecular oxygen. In its ground state, molecular oxygen contains two unpaired electrons. As such, it interacts with any introduced spin probes via collisional spin exchange. The interdependence of oxygen concentration on the relaxation rate of the corresponding ESR signal makes it possible to measure the partial pressure of oxygen in tissues with high resolution.

Another key biomedical application of ESR is in the measurement of radiation exposure, also known as dosimetry. This is because ionizing radiation creates free radicals in living tissues. Materials such as tooth enamel, fingernails, and bone can retain radiation-induced radicals for long periods. This makes it possible to obtain radiation dose assessments retrospectively. While these developments remain in their early states, recent in vivo ESR technology advances now enable non-invasive dosimetry directly on living organisms which will be a powerful clinical tool, particularly in the context of large-scale radiation exposure events.[7]

ESR can also be used in non-invasive medical imaging. Much like the well established technique of using NMR for imaging, electron paramagnetic resonance imaging (EPRI) also uses magnetic field gradients and radiofrequency pulses to create maps of spin probe distribution in tissues. However, due to the higher gyromagnetic ratio of electrons in comparison to a nucleus, EPRI operates at lower magnetic fields than MRI. This makes it highly sensitive to free radical concentrations which, given its power to investigate tumor microenvironments, oxygen gradients, and redox status in living subjects, serves as a modality that might be comparable to to MRI in cancer and metabolic disease research.[8,9]

Finally, central to the ESR setup is the resonator, which couples microwave energy into the sample to drive spin transitions.[10] The Collett Lab utilizes a loop-gap resonator (LGR), a design that has also been used in various biomedical ESR applications.[11,12] Given this overlap, future work could explore whether the current resonator systems in the Collett Lab might be adapted for biological spin measurements, such as those used in EPR oximetry or EPR imaging.

ESR spin-labelling techniques also allow detection and identification of radical species. This makes it

possible to direct studies of oxidative damage and thus track the efficacy of related therapeutic interventions.[13] This ability to detect transient changes in radical species in real time and quantify changes in tissue oxygenation make ESR an invaluable tool whose clinical applications certainly warrant further exploration.[6] These applications show how the direct detection of radicals via ESR might bridge a critical gap in medical diagnostics and molecular biology—and its potential as a non-invasive, quantitative, and real-time measurement of redox dynamics in health and disease.[6] These applications illustrate the significant biomedical potential of ESR beyond basic spectroscopy. They also highlight opportunities for novel instrumentation and pulse techniques that can expand the relevance of ESR in clinical research.

4 Theory

4.1 Hamiltonian

As discussed in the background section, our system is a model of two spin labels, both of which are spin $\frac{1}{2}$ particles. A static magnetic field $\vec{B_0}$ is applied in the $\hat{z}$ direction and an oscillating radio frequency (RF) field $\vec{B_1}(t)$ is also present in the $\hat{y}$ direction.

$$\vec{B}(t) = \vec{B_0} + \vec{B_1} = B_0\hat{z} + 2B_1 cos(\omega_1 t)\hat{x} \tag{1}$$

The energy levels of a system are described by the Hamiltonian operator. For our two spin system, the Hamiltonian has three components: $\mathscr{H}_Z$ from the Zeeman interaction with the static field $\vec{B_0}$, a coupling term $\mathscr{H}_J$, and a radio frequency (RF) term from the oscillating field.

Though we will break down each individual term in the following derivations, the total Hamiltonian used for our spin system is

$$\mathscr{H} = \mathscr{H}_Z + \mathscr{H}_J + \mathscr{H}_{RF} \tag{2}$$

4.2 Zeeman interaction term

The Zeeman term due to spin interacting with the static field B_0 is

$$\mathscr{H}_Z = -\vec{\mu} \cdot \vec{B_0} = g\mu_B B_0 S_z = \hbar\omega_0 S_z \tag{3}$$

with oscillation frequency $\omega_0 = \frac{g\mu_B B_0}{\hbar}$. The magnetic moment is given by

$$\vec{\mu} = g\mu_B \vec{S}$$

where μ_B represents the Bohr magneton and g is a dimensionless constant that relates the magnetic dipole moment of an electron spin to its angular momentum. The g value for an isolated electron is 2, however, that changes significantly depending what spin label is in use.

Note that because we are looking at a two-spin system, the total Zeeman term will have contributions from both S_{z_1} and S_{z_2}. Taking that into account, equation 3 can be expanded as

$$\mathscr{H}_Z = -\mu \cdot \vec{B_0} = g\mu_B B_0(S_{z_1} + S_{z_2}) = \hbar\omega_0(S_{z_1} + S_{z_2}) \tag{4}$$

4.3 RF Hamiltonian for ESR

The radio-frequency (RF) term $\mathscr{H}_{RF}$ then describes interactions with the oscillating transverse field $\vec{B}_1$:

$$\mathscr{H}_{RF}(t) = -\vec{\mu} \cdot \vec{B}_1(t) = 2\mu_B B_1 cos(\omega t + \phi) g S_x \tag{5}$$

where t is time, ω is the frequency of the RF field in the xy plane, and ω_0 is the Larmor precession frequency along the static field B_0. The phase shift given by ϕ dictates the orientation of the oscillating field in the transverse plane, and thus the axis about which the spin rotates in the rotating frame.[14]

The transverse nature of $\mathscr{H}_{RF}$ is what ultimately drives spin state transitions in our a system. The applied RF field must be perpendicular to B_0 to drive time-dependent transitions that do not commute with the static Hamiltonian.

While the RF field is applied, the spins will be oscillating between states at the Rabi frequency which is defined as

$$\Omega_1 = \frac{g\mu_B B_1}{\hbar} \tag{6}$$

where g is the electron g factor, μ_B is the Bohr magneton, B_1 is the oscillating field amplitude in the $\hat{y}$ direction, and $\hbar$ is the reduced Planck constant.[15]

With equations 3 and 5, we can re-express equation 2 as the standard ESR Hamiltonian due to the application of both static and oscillating fields in the $\hat{z}$ and $\hat{y}$ directions respectively. As we will discuss later, the RF field will only be applied for some of the time.

$$\mathscr{H}(t) = \hbar\omega_0 S_z + \hbar\Omega_1 cos(\omega t) S_y \tag{7}$$

4.4 Rotating Wave Approximation (RWA)

The RF Hamiltonian from equation 7 can be further simplified by transforming into a frame rotating at the frequency ω of the oscillating field. We will be simulating an ensemble of spins with slightly varying precession rates to model the local field inhomogeneities that are typically present. In this rotating frame, rapidly oscillating terms in the lab frame Hamiltonian are averaged out, yielding an approximation with no temporal dependence. Using Euler's relation, the cosine term in the RF field can be rewritten as

$$cos(\omega t) = \frac{1}{2} e^{-i\omega t}$$

. Under the rotating wave approximation (RWA), the counter-rotating term $e^{i\omega t}$ can be neglected since it

averages to zero over relevant timescales. Substituting into equation 7, we obtain a simplified expression for our rotating frame Hamiltonian:

$$\mathscr{H}_{RWA} = \hbar(\omega_0 - \omega)S_z + \frac{1}{2}\hbar\Omega_1 S_x \tag{8}$$

The first term captures the decoherence of the system which is defined as the frequency difference between the spin's natural precession rate ω_0 and the RF field frequency ω. When $\omega = \omega_0$, the RF field is oscillating at its resonance frequency and the detuning term vanishes. However, due to local field inhomogeneities, slight decoherence often exists in practice which can have significant effects on spin dynamics. In real samples, static magnetic fields can experience slight variations in different spin environments. This can cause each spin to precess at a frequency that is slightly different than ω_0. Consequently, some spins are precessing slightly faster and others slower than the RF field which, in the rotating frame, leads to destructive interference as spins gradually spread out. The resultant decrease in net magnetization is a major contributor to transverse decoherence and is quantified by the time constant T_2 (not the same as spin-spin interactions). The rotating frame Hamiltonian in equation 8 is the effective model we ultimately use in our simulations to describe spin dynamics under pulsed ESR conditions.

4.5 Decoherence

In any realistic spin system, interactions with the surrounding environment lead to decoherence—the gradual loss of quantum phase information over time. While the Hamiltonian in equation 2 governs the unitary evolution of an isolated spin system, decoherence introduces non-unitary dynamics that must be considered to accurately model experiments such as DEER.[15]

One of the primary sources of decoherence in pulsed ESR experiments arises from fluctuations in the local magnetic field, which can be caused by inhomogeneities due to molecular motion, spin-lattice interactions, or other nearby paramagnetic species.[2] These random fluctuations lead to a spread in precession frequencies, causing spins to dephase relative to each other over time. Importantly, in the context of DEER, we rely on controlled fluctuations of the local field due to intentional flipping of the second spin which is how changes to the precession behavior of spin 1 are induced.

Although including decoherence in the simulation is somewhat straightforward (ie. adding T_2 relaxation terms), our purpose in this work is to verify the correct modeling of the coherent distance-measurement process in DEER. As such, we assume a closed quantum system to isolate spin-spin interaction effects in an idealized system. This means we neglect environmental interactions and treat the system as undergoing exclusively unitary evolution. This assumption simplifies the analysis and highlights the role of dipolar coupling and pulse sequences in generating and detecting DEER oscillations.

The rotating wave approximation given in equation 8 is the total spin Hamiltonian ultimately used for the purpose of our simulation.

4.6 Dipolar Interaction Term

For the two interacting spins in our system, we must account for their dipole-dipole coupling in the total Hamiltonian. Their interaction is sensitive to the inter-spin vector $\vec{r} = |r|\hat{r}$ where $|r|$ is the magnitude of the spin-spin separation and $\hat{r}$ points from one spin to the other and thus can be used to extract the distance between the two spins in the system.

The classical dipole-dipole interaction energy between two magnetic dipoles is given by

$$E_d = \frac{\mu_0}{4\pi r^3} \left[\vec{\mu}_1 \cdot \vec{\mu}_2 - 3(\vec{\mu}_1 \cdot \hat{r})(\vec{\mu}_2 \cdot \hat{r}) \right], \tag{9}$$

where μ_0 is the vacuum permeability $\vec{r}$ is the inter-spin vector. Substituting the expressions for $vec\mu_1$ and $\vec{\mu}_2$, we obtain the dipolar interaction Hamiltonian:

$$\mathscr{H}_J = \frac{\mu_0}{4\pi} \frac{g_1 g_2 \mu_B^2}{r^3} \left[\vec{S}_1 \cdot \vec{S}_2 - 3(\vec{S}_1 \cdot \hat{r})(\vec{S}_2 \cdot \hat{r}) \right]. \tag{10}$$

To extend this discussion to DEER, we focus on how the dipolar interaction $\mathscr{H}_J$ provides a mechanism for measuring distances between spin labels. As shown in equation 10, the strength of the dipolar coupling scales as $1/r^3$, where $|r|$ is the distance between the two spins.

In a DEER (Double Electron-Electron Resonance) experiment, this dipolar interaction causes modulations in the spin echo signal. Specifically, spin 1 is manipulated with a standard spin echo sequence, while a second spin is flipped by a separate pulse at a different frequency in the transverse direction. When the pump pulse flips the state of the second spin, the local dipolar field experienced by the first spin changes, which in turn alters its precession and changes the amplitude of the echo signal. These modulations encode the strength of the dipolar interaction from which the inter-spin distance can be extracted.

The oscillation frequency in the resulting DEER signal can then be used to extract the dipolar coupling constant D. This relates to the distance between spins $|\vec{r}|$:

$$D = \frac{\mu_0}{4\pi} \cdot \frac{g_1 g_2 \mu_B^2}{\hbar r^3} (1 - 3\cos^2\theta), \tag{11}$$

where θ is the angle between the inter-spin vector $\vec{r}$ and the static magnetic field $\vec{B_0}$. The orientation dependence is in the term $1 - 3\cos^2\theta$.

In systems with randomly oriented spin pairs, like our simulation environment, molecules adopt random orientations with respect to static field B_0.[16] The orientation-dependent term, $1 - 3\cos^2\theta$ from equation 11 cancels out and the resulting signal depends only on the inter-spin distance distribution $\vec{r}$.

We model both the coherent dynamics of spin evolution with and without applied radio frequency fields but are only simulating the simplified version of the spin system. This allows us to investigate how different dipolar couplings might alter recorded echo intensities and how they evolve as a function of time T.

Changes to the echo signal due to the dipolar interaction between the two electron spins $V(t)$, can be expressed as:

$$V(t) = \int_{R_{\min}}^{R_{\max}} \kappa(r,t) P(r)\, dr \tag{12}$$

Where $P(r)$ is the distance distribution function, and $\kappa(r,t)$, the most general form of the coupling term, is:

$$\kappa(r,t) = \int_0^1 \cos\left[(1-3x^2)\omega_d t\right]\, dx \tag{13}$$

with dipolar coupling frequency

$$\omega_d = \frac{\mu_0}{4\pi}\frac{g^2\mu_B^2}{\hbar r^3}$$

. Here, $x = \cos(\theta)$, and θ is the angle between the inter-spin vector $\vec{r}$ and the external magnetic field direction.[17]

In our simplified model, we assume a single, fixed distance between spins and a specific orientation ($\theta = \pi/2$), which simplifies equation 13 to:

$$\kappa(r,t) = \cos(\omega_d t) \tag{14}$$

This assumption corresponds to adjacent spins in the transverse (xy) plane. As will be discussed in the following sections, resultant modulation pattern in the DEER signal can then be used to calculate the distances between spin labels.

5 Methods

5.1 Pulse Sequence

The Hahn echo sequence is a fundamental technique in pulsed magnetic resonance experiments, designed to mitigate the effects of inhomogeneous broadening in spin systems.

The typical 4-pulse DEER sequence used in this experiment consists of the following steps:

1. **Initial $\pi/2$ pulse**: This pulse tips the net magnetization vector from its equilibrium position along the static magnetic field B_0 (for our specific spin system this is in the $+\hat{z}$ direction) into the transverse (xy) plane. The resulting superposition of spin states is what then initiates precession at their respective Larmor frequencies.[18]

2. **Evolution period τ**: During this interval, spins de-phase due to local magnetic field inhomogeneities, leading to a decay in the observable transverse magnetization.

3. **Refocusing π pulse**: Applied after time τ, this pulse inverts the spin vectors in the transverse plane to refocus the spins due to any decoherence that occurred due to static inhomogeneities in the prior relaxation period

4. **Echo formation at time 2τ**: After an additional period τ, the spins re-cohere which results in the formation of a spin echo. The additional period is necessary because the system is initially overwhelmed by the pulse ringdown. Following the evolution period, spins re-align which we can detect because our equipment is sensitive to oscillating fields in the transverse plane. As such,any decoherence that occurred due to static field inhomogeneities are effectively refocused. This allows for a more accurate measurement of spin-spin relaxation times (T_2).[19]

Building upon the Hahn echo sequence, the four-pulse Double Electron-Electron Resonance (DEER) sequence introduces additional pulses to measure dipolar interactions between electron spins, providing insight into distances at the nanometer scale. The sequence is as follows:

1. **Spin 1 $\pi/2$ pulse**: Initial state of spin ensemble; spins are aligned with net magnetization vector $\vec{B_0}$ in the $+\hat{z}$ direction.

2. **First evolution period τ**: Spins dephase due to inhomogeneities.

3. **Spin π pulse**: Inverts the spins, initiating rephasing.

4. **Second evolution period τ**: Spins continue to evolve, leading to the formation of an echo at time 2τ.

5. π **pulse on spin 2**: Applied at a different frequency, this pulse selectively inverts a second set of spins (spin 2) at a variable time T after the initial $\pi/2$ pulse. The dipolar interaction between the spin 1 and spin 2 causes a modulation in the echo amplitude as a function of T.

6. **Spin 1** π **pulse**: A second π pulse applied to spin 1 which refocuses the echo. This increases the dipolar interaction sensitivity.

This sequence allows for the measurement of dipolar coupling between spins, which is directly related to the distance between them as described in more detail in the theory section. By analyzing the modulation of the echo amplitude as a function of the spin 2 delay, a sinusoidal curve fit in equation 20 can be applied. The parameters one can extract distance distributions within the sample.[20]

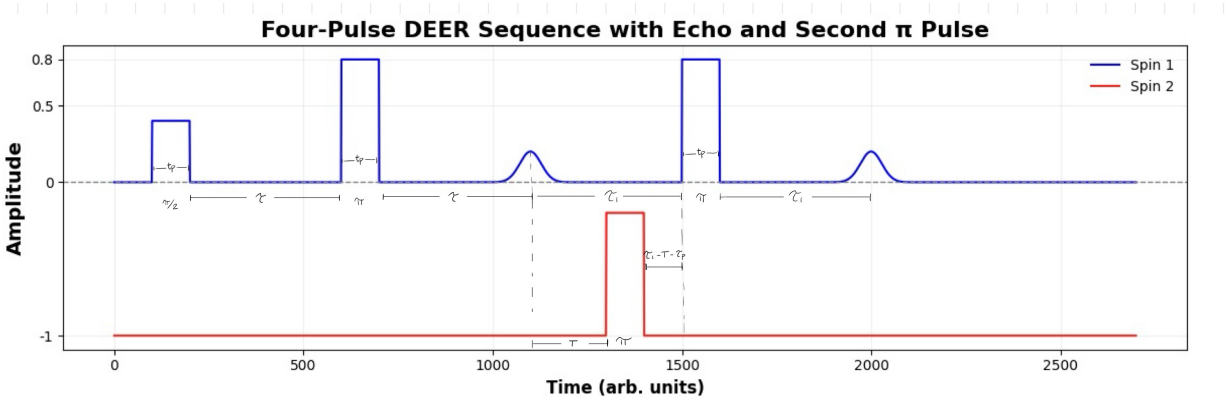

Figure 1: Schematic of the four-pulse DEER sequence. The spin 1 pulses (black) create and refocus the spin echo, while the spin 2 (red) inverts the spins at a variable time T. The echo amplitude is modulated due to dipolar interactions.

5.2 Bloch Sphere time evolution

Spin ensemble simulation: The spin ensemble progression in response to the DEER pulse sequence is shown in figure 2. (a) shows the spin ensemble in its ground state where the spins are aligned with the static magnetic field along the $+\hat{z}$ axis. (b) shows the evolved ensemble state after the initial $\pi/2$ pulse. After evolution period τ, spins in the ensemble are coherently aligned with the x-axis. After time τ, spins in the ensemble spread out in the xy plane due to local field inhomogeneities (c). As shown in (d), π pulse is then applied and spins are inverted about the transverse (xy) plane. This initiates echo formation which occurs at time 2τ (e). The time evolution of the system at time τ after the aforementioned echo is shown in (f). A second π pulse is applied to spin 1 which again, inverts the spins (g) which initiates a second echo (e) occurring at time 2τ after first echo.

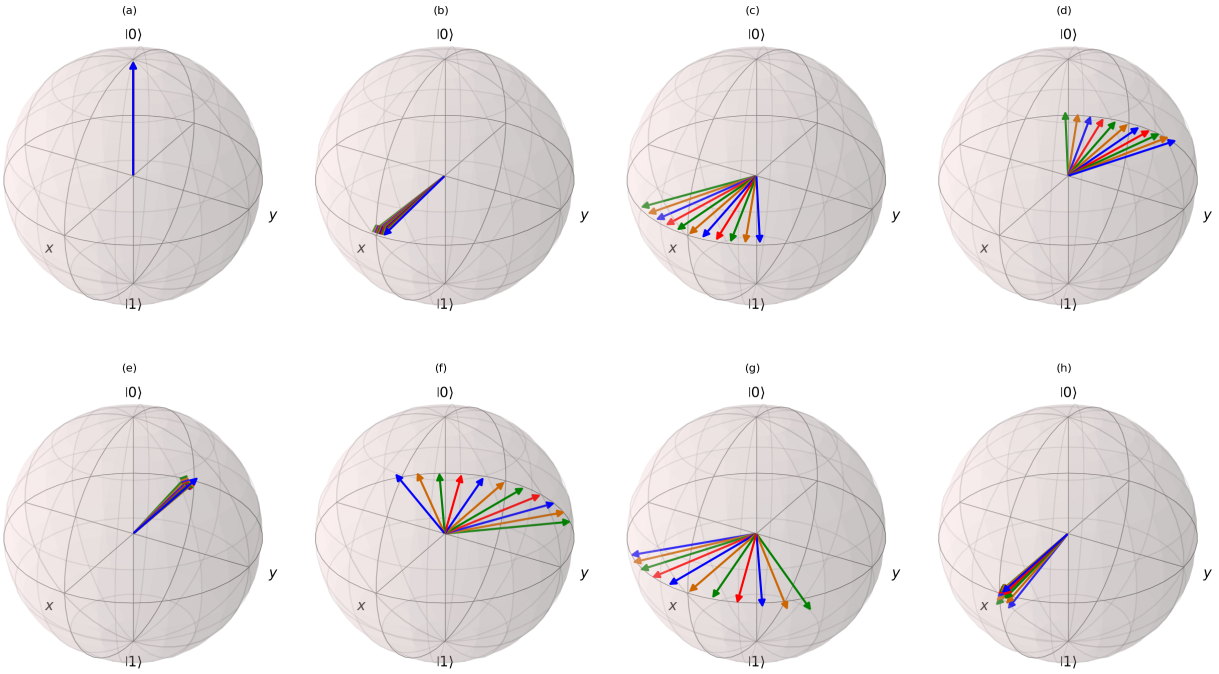

Figure 2: Ensemble state after evolution period due to each spin 1 pulse in the 4-pulse DEER sequence seen in figure 1. Each sphere represents the ensemble state after the associated time evolution period.

5.3 Qutip Simulation Framework

All analyses presented here are based on simulations of a two-spin system, rather than experimental measurements. We employ the Quantum Toolbox in Python (QuTiP) to simulate the dynamics of spin systems under the four-pulse DEER (Double Electron-Electron Resonance) sequence. QuTiP facilitates the construction of time-dependent Hamiltonians and the numerical integration of the Schrödinger equation to model the time evolution of a closed quantum system. This is made possible by QuTiP's master equation solver function, `mesolve`, which numerically integrates the following equation:

$$i\hbar \frac{d}{dt}|\psi(t)\rangle = \hat{H}(t)|\psi(t)\rangle \tag{15}$$

Collapse operators are set equal to an empty list and consequently, `mesolve` defaults to solving the standard time-dependent Schrödinger equation. This models unitary evolution, which is appropriate for closed quantum systems like that of our simulation environment.[21] In this scenario, the system's evolution is solely determined by its Hamiltonian, without no energy dissipation.

The total Hamiltonian $\hat{H}(t)$ as shown in equation 2, is composed of multiple components:

$$\hat{H}(t) = \hat{H}_{\text{Zeeman}} + \hat{H}_{\text{RF}}(t) + \hat{H}_{\text{dipolar}} \tag{16}$$

- **Static Zeeman Term** ($\hat{H}_Z$): Represents the interaction of each spin with the external static magnetic field.
- **Radiofrequency (RF) Term** ($\hat{H}_{RF}(t)$): Time-dependent terms corresponding to the applied microwave pulses
- **Dipolar Interaction Term** ($\hat{H}_{\text{dipolar}}$): Accounts for dipole-dipole coupling between the two electron spins

Defining the pulse sequence and corresponding parameters within QuTiP is what allows us to model and predict the resulting echo signals of our two-spin system.

5.4 Dipolar Interaction and Distance Extraction

To extract the dipolar coupling frequency ω_d from the simulated echo signal, we fit the modulation to a damped cosine function:

$$V(T) = Ae^{-BT}\cos(CT + D) + E \tag{17}$$

Here, C corresponds to ω_d. Once ω_d is determined, the inter-spin distance r can be calculated using:

$$r = \left(\frac{\mu_0}{4\pi}\frac{g^2\mu_B^2}{\hbar\omega_d}\right)^{1/3} \tag{18}$$

This is the approach that ultimately allows us to simulate DEER experiments and extract quantitative distance information between spins based on the dipolar interaction.

6 Results

As derived in the theory section, the total spin Hamiltonian in the rotating frame used in our simulation is

$$\mathscr{H} = \mathscr{H}_Z + \mathscr{H}_J + \mathscr{H}_{RF}. \tag{19}$$

For the purposes of our simulated $V(T)$ plot shown below (see figure 3), each term is simplified such that precession rates about the $+\hat{z}$ axis are only being accounted for in the Zeeman interaction term $\mathscr{H}_Z = \vec{r} S_{Z_1}$. We simulate an ensemble of $N = 100$ spins with varied precession rates from -5 to $+5$ GHz.

Simulation parameters used are shown in the following table:

Parameter	**Symbol**	**Value**	**Units**
Pulse width	t_p	$\pi/2$	ns
Delay time (fixed)	τ	5	ns
Delay time (variable)	τ_1	10	ns
Dipolar coupling strength	$J_{\|}$	0.5	GHz
RF pulse strength	ω_1	1	GHz

Table 1: Simulation parameters used in the total DEER spin Hamiltonian. Note that the variable delay time is the maximum offset used for figure 3.

To characterize the effect of dipolar coupling between electron spins, we simulated a DEER pulse sequence with a variable delay time T. The overlap between the final state and a reference state—defined as the uncoupled state following the pulse sequence—can act as a proxy for the echo signal. As such, varying the delay time makes it possible to observe how spin-spin interactions affect the overall coherence of the system.

6.1 V(T) modulation from dipolar coupling

In our simulations, we varied the delay time T from 0 to $\tau_1 - t_p$, where, as shown in figure 1, t_p is the duration of the π pulse acting on spin 2. For each T value, the average overlap between its final evolved spin state and its known initial state is then used to obtain $V(T)$ shown in figure 3. The oscillatory signal observed reflects coherent spin-spin coupling.

These oscillations arise from the time evolution caused by the dipolar interaction during the delay periods before and after the spin-2 π pulse. As detailed in the theory section, this interaction introduces a phase shift that is dependent on the dipolar coupling constant, which in turn depends on the inter-spin vector $\vec{r}$.

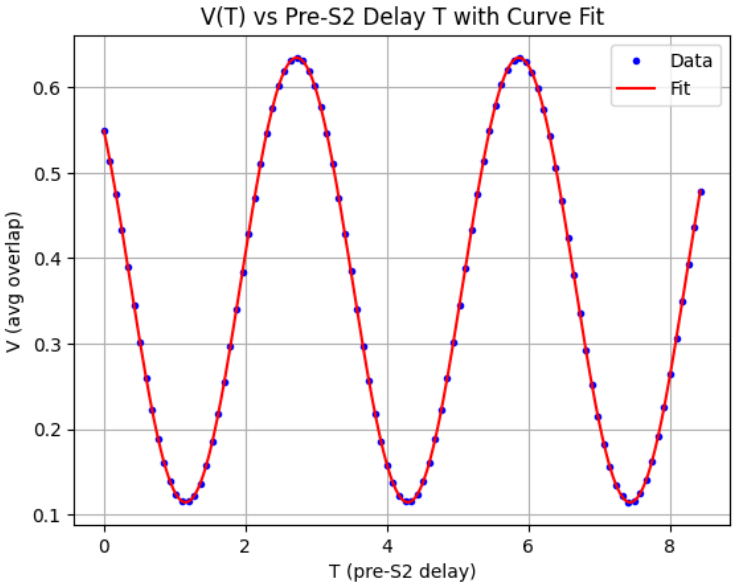

Figure 3: V(T) plot with sinusoidal curve fit (see equation 20). Fit parameters for our simulated data set are shown in table 2

The damped oscillatory behavior of our curve fit from figure 3 is accomplished using the following function:

$$V(T) = Ae^{-BT}\cos(C \cdot T + D) + E \tag{20}$$

for which A is the oscillation amplitude, B is the decay rate, C is the dipolar frequency, D is the phase shift, E is the vertical offset, and time T is measured in nanoseconds. The only distance dependent parameter is the dipolar frequency C.

Table 2: Fitted Parameters for $V(T)$ Curve with Standard Errors and Units

Parameter	**Value ± Uncertainty**	**Units**
A	0.260 ± 0.015	A.U
B	0.000 ± 0.002	ns^{-1}
C	2.000 ± 0.020	ns^{-1}
D	0.833 ± 0.010	Radians
E	0.374 ± 0.012	A.U

The distance distribution is contained in the dipolar frequency which corresponds to the fit parameter $C = 2.000$ GHz. The inter-spin distance $|r|$ can then be extracted via the dipolar coupling relationship derived in equation 11.

$$\omega_d = \frac{\mu_0 g^2 \mu_B^2}{4\pi\hbar r^3} \quad \Rightarrow \quad r = \left(\frac{\mu_0 g^2 \mu_B^2}{4\pi\hbar\omega_d}\right)^{1/3}$$

Substituting physical constants and dipolar frequency $\omega_d = 2.000$ GHz, we obtain an inter-spin distance:

$$r \approx 2.5\text{nm}$$

This result demonstrates how DEER spectroscopy can resolve spin-spin distances on the nanometer scale, validating the simulation approach.

7 Discussion

This simulation demonstrates how varying the timing of a spin-selective π pulse in a DEER sequence allows the extraction of dipolar oscillation frequencies from which the distance between two coupled spins can be obtained. By fitting the simulated echo signal to a damped cosine function, we obtained a quantitative measure of the dipolar coupling strength, and thereby the inter-spin distance. This supports the use of DEER as a model-based tool for simulating and analyzing spin dynamics in coupled systems.

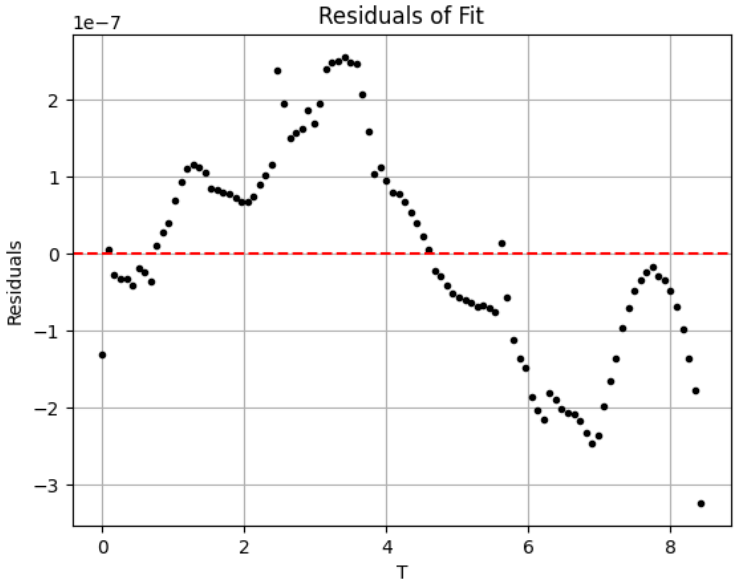

Figure 4: Residuals of the fitted curve V(T) from Equation (20), showing the difference between the simulated data and the fitted model. The small residual values indicate a good fit and validate the accuracy of the damped oscillatory function

Shown in figure 4 are the $V(T)$ residuals. This represents the differences between observed data and what is predicted by our fitted function from equation 20 and fit parameters shown in table 2. Our residuals are on the order of $1e^{-7}V$ while the actual signal oscillations are on the order of $1e^{-1}V$. The fractional error of $1e^{-5}$ indicates an excellent fit for this data set.

At this point, the main contributor to the error is likely the slight decoherence incorporated through the precession rates. This is because after the pulses all the spins are not completely aligned, and that inevitably

introduces some error. At this point, this is not particularly meaningful given that our simulation is so close to that of an ideal model. Still, the dataset produced is a good fit to the anticipated function which indicates that, at a fundamental level, our simulation is successfully modeling a two spin system.

A possible way to proceed in this project would be to extend the simulation to incorporate some environmental effects that would typically be present in an open quantum system. The most immediate next step would be to make the coupling more complicated which would better model how a true pair of spin labels would be behaving in practice. The additional ideas listed above—environmental effects, pulse variations, and different labeling strategies—are also valuable and should be pursued in future work. Additionally, exploring different pulse timings, pulse shapes (ie. continuous wave as opposed to pulsed excitation), and spin labels could improve the resolution and biological relevance of the simulation. The existing framework can be used to account for how the resultant relaxation effects might impact the distribution of spin–spin distances.

8 Conclusion

In this project, we used simulations to explore the principles and capabilities of Double Electron-Electron Resonance (DEER) spectroscopy, a pulsed ESR technique for measuring nanoscale distances between spin labels.[4,22] DEER distance measurements are increasingly relevant to structural studies of biological molecules such as proteins, nucleic acids, and membranes.[16] By modeling a two-spin system with variable dipolar coupling and precession rates, we implemented a four-pulse DEER sequence using the Quantum Toolbox in Python (QuTiP),[23] and analyzed the resulting echo modulation as a function of the delay time between pulses. Fitting the simulated echo signals allowed us to extract characteristic oscillation frequencies directly related to the dipolar interaction strength, and therefore to inter-spin distance.[16] These results support the expected relationship between DEER signal modulations and nanoscale structural information.Our simulation framework provides a basis for extending DEER analysis to more complex spin systems and incorporating realistic experimental effects such as noise, orientation selection, and relaxation dynamics.[20] The simulations detailed in this project can advance the general understanding of spin labels and how they might inform future DEER experiments.

A Code Listings

Below are key scripts used for the simulation and $V(T)$ plot generation as well as Bloch sphere visualization using QuTiP and `matplotlib`.

A.1 Pulse and Evolution Functions

```
import qutip as qt
import numpy as np

Sz1 = qt.tensor(qt.sigmaz(), qt.qeye(2))
Sz2 = qt.tensor(qt.qeye(2), qt.sigmaz())
Sy1 = qt.tensor(qt.sigmay(), qt.qeye(2))

def pulse(in_states, precession_rates, pulse_time, J_par=0, show_Bloch=True):
    # ... code content ...
    return evolved_states0
```

Listing 1: Core pulse and evolution functions

A.2 V(T) Curve Generation

```
# Constants
t_p = np.pi / 2
tau = 5
tau_1 = 10
J_par = 0.5

T_values = np.linspace(0, tau_1 - t_p, 100)
V_values = []

for T in T_values:
    # Pulse sequence
    # ... code content ...
    V_values.append(V)

plt.plot(T_values, V_values)
plt.xlabel('T')
plt.ylabel('V(T)')
```

Listing 2: Simulation loop for V(T) curve

References

[1] Yu Fang and et al. Free radicals in biology and medicine. *Free Radical Biology and Medicine*, 150:1–17, 2020.

[2] Charles P. Slichter. *Principles of Magnetic Resonance*. Springer, 1990.

[3] Charles P. Poole. *Electron Spin Resonance: A Comprehensive Treatise on Experimental Techniques*. Dover Publications, 1996.

[4] Gunnar Jeschke. Deer distance measurements on proteins. *Annual Review of Physical Chemistry*, 63:419–446, 2012.

[5] Lien Ai Pham-Huy, Hua He, and Chanin Pham-Huy. Free radicals, antioxidants in disease and health. *International journal of biomedical science: IJBS*, 4(2):89–96, 2008.

[6] Harold M Swartz, Benjamin B Williams, Bassem I Zaki, Alan C Hartford, Lesley A Jarvis, Eunice Y Chen, Richard J Comi, Marc S Ernstoff, Huagang Hou, Nadeem Khan, et al. Clinical epr: unique opportunities and some challenges. *Academic radiology*, 21(2):197–206, 2014.

[7] B. B. Williams and et al. In vivo epr dosimetry: Radiation dose measurements using epr signals in teeth. *Applied Radiation and Isotopes*, 52(5):1031–1038, 2000.

[8] D. J. Lurie, M. A. Foster, D. Yeung, and J. M. S. Hutchison. Development of epr in vivo imaging. *Physica Medica*, 21:10–15, 2005.

[9] Valery V. Khramtsov and Jay L. Zweier. Quantitative in vivo oxygen imaging with epr. *Antioxidants & Redox Signaling*, 12(5):793–816, 2010.

[10] George A. Rinard and Gareth R. Eaton. Loop-gap resonators. In Sandra S. Eaton, Gareth R. Eaton, and Lawrence J. Berliner, editors, *Biomedical EPR Part B: Methodology, Instrumentation, and Dynamics*, volume 24 of *Biological Magnetic Resonance*, pages 19–52. Springer US, Boston, MA, 2005.

[11] Craig McHugh and Harold M Swartz. Biomedical epr imaging. *Journal of Magnetic Resonance*, 213:389–393, 2011.

[12] Jan H Ardenkjaer-Larsen, Ib Laursen, Inge Leunbach, Gunnar Ehnholm, Lars-Gunnar Wistrand, Jonas S Petersson, and Klaes Golman. Developments in epr instrumentation for biomedical and pharmaceutical applications. *Journal of Magnetic Resonance*, 162:219–227, 2003.

[13] Ashutosh Kumar Shukla and Ashutosh Kumar Shukla. *Electron Spin Resonance Spectroscopy in Medicine*. Springer, 2019.

[14] John S Townsend. *A modern approach to quantum mechanics*. University Science Books, 2000.

[15] Malcolm H. Levitt. *Spin Dynamics: Basics of Nuclear Magnetic Resonance*. John Wiley & Sons, 2nd edition, 2008.

[16] Peter P. Borbat and Jack H. Freed. Pulsed dipolar esr: Distance measurements in biomacromolecular systems. In *Methods in Enzymology*, volume 423, pages 52–116. Academic Press, 2007.

[17] Ilya Kuprov, Janet E. Lovett, and P. J. Hore. Time domain simulation of gd^{3+}–gd^{3+} distance measurements by epr. *Journal of Magnetic Resonance*, 275:1–10, 2017.

[18] Jürgen Hennig. Echoes—how to generate, recognize, use or avoid them in mr-imaging sequences. *Concepts in Magnetic Resonance*, 3(3):125–143, 1991.

[19] Arthur Schweiger and Gunnar Jeschke. *Principles of Pulse Electron Paramagnetic Resonance*. Oxford University Press, 2001.

[20] Gunnar Jeschke and Yevhen Polyhach. Distance measurements in biological systems by epr spectroscopy. *Physical Chemistry Chemical Physics*, 4(3):527–535, 2002.

[21] QuTiP Development Team. *Solving Problems with Time-dependent Hamiltonians - QuTiP*, 2025.

[22] A. D. Milov, A. B. Ponomarev, and Yu. D. Tsvetkov. Electron-electron double resonance in electron spin echo: Model biradical systems and the sensitized photolysis of decalin. *Chemical Physics Letters*, 110(1):67–72, 1981.

[23] J R Johansson, P D Nation, and F Nori. Qutip 2: A python framework for the dynamics of open quantum systems. *Computer Physics Communications*, 184(4):1234–1240, 2013.